Evaluation of silver nanostructures fabricated using glancing angle deposition as localized surface plasmon resonance biosensors

D.A. Gish*, F. Nsiah**, M.T. McDermott** and M.J. Brett*

* Department of Electrical and Computer Engineering, University of Alberta
Edmonton, Alberta, Canada T6G 2V4, dgish@ualberta.ca
** Department of Chemistry and National Institute for Nanotechnology
University of Alberta, Edmonton, Alberta, Canada T6G 2G2

ABSTRACT

Localized surface plasmon resonance based biosensors were fabricated from silver nanoparticle films produced by glancing angle deposition. The films were approximately 150 nm thick, and exhibited a strong extinction peak around 368 nm in air. The position of the extinction peak red-shifted with increasing refractive index of the surrounding medium. The films were functionalized with 11-amino-1-undecanethiol and rabbit immunoglobulin G (rIgG) to allow for the detection of anti-rIgG binding. The wavelength shift at varying concentrations of anti-rIgG was measured and fit to the Langmuir isotherm, from which we obtained values for the saturation response, 29.4 $\pm$ 0.7 nm, and the surface confined binding constant, (2.7 $\pm$ 0.3) $\times$ 10^6 M^{-1}. The response of the sensors to nonspecific binding was also investigated.

Keywords: silver nanoparticles, localized surface plasmon resonance, biosensor, glancing angle deposition

1 INTRODUCTION

The optical response of noble metal nanoparticles is typically characterized by the presence of a strong absorption and scattering peak that is not present in the spectrum of the bulk metal. This phenomenon, known as localized surface plasmon resonance (LSPR), is due to the coupling of the conduction electrons in the metal to the electromagnetic field of the incident light. The resonance position is dependent on the size and shape of the particles, coupling between the particles, the dielectric properties of the metal, and the dielectric properties of the local environment surrounding the particles [1]. There has been a lot of recent interest in applications based on LSPR, particularly for use as refractive index sensors [2–15]. By measuring shifts in the extinction peak position, changes in the refractive index near the particle surface can be detected. Functionalizing the surface of the nanoparticles to bind to a specific analyte allows for sensitive and selective biosensors to be designed.

In this study, glancing angle deposition (GLAD) was used to fabricate silver nanoparticle films that are evaluated for LSPR biosensing. Glancing angle deposition is a single-step deposition process utilizing oblique angle physical vapour deposition combined with precision substrate rotation [16–18]. Using GLAD, the morphology of thin films can be tailored on nanometre size scales by exploiting the self-shadowing effects that arise when vapour flux arrives at highly oblique angles to the substrate surface. The binding event of anti-rabbit immunoglobulin G (anti-rIgG) to rabbit IgG (rIgG), which is attached to the nanoparticle surface, is detected.

2 EXPERIMENTAL

2.1 Sample Fabrication

The silver nanoparticles used in this study were fabricated by glancing angle deposition using an electron beam evaporation system. Prior to deposition, $1'' \times 1''$ fused silica substrates were cleaned using Citranox cleaner from Alconox, Inc. (White Plains, New York). The substrates were loaded on a motor controlled substrate holder located 42 cm above the electron beam crucible. The vapour source material was silver shot from Cerac (Milwaukee, Wisconsin) with a purity of 99.99%. The chamber was evacuated to a base pressure of 1.5×10^{-5} Pa by cryogenic pumping. Deposition of the silver was carried out at a pressure of 1.3×10^{-4} Pa.

In the GLAD technique, the substrate orientation is described by the angle, α, between the crucible normal and the substrate normal, and the angle of rotation, ϕ, about the substrate normal. For this study, the substrates were held at an oblique angle, α, of 85°, while ϕ was constantly rotated at a rate of one revolution for every 3 nm of film growth. The deposition rate was measured by a quartz crystal microbalance (QCM) and was kept at 1 Å/s. The the film was grown to a thickness of approximately 150 nm. The samples were stored in a nitrogen environment.

2.2 Sensitivity Measurements

To evaluate the sensitivity of the films to changes in the refractive index of their environment, extinction spectra of a sample were measured while immersed in liquids of various refractive indices. The liquids used were deionized water, 2-propanol, and chloroform with refractive indices of 1.33, 1.38, and 1.45, respectively.

2.3 Biosensor Preparation and Testing

Prior to biosensor preparation, the extinction spectrum of the sample was measured. The sample was then soaked overnight in 2 mM 11-Amino-1-undecanethiol (11-AUT) in water from Dojindo Laboratories (Japan). The extinction spectrum was measured again after the sample was rinsed in deionized water and dried under nitrogen flow. Next the sample was immersed in 6.7 μM rabbit immunoglobulin G (rIgG) in 1 mM phosphate buffered saline (PBS), pH=7.4, for 1 hour. Following this, the sample was first rinsed with 1 mM PBS to wash away unbound proteins, and then deionized water to prevent salt deposits from forming. Finally, the sample was dried under nitrogen flow before taking another extinction spectrum measurement.

To test the biosensor, a sample which was functionalized with 11-AUT and rIgG was immersed in varying concentrations of polyclonal (goat) anti-rIgG. Each immersion lasted for 1 hour and proceeded from the lowest concentration of 13 nM up to a maximum concentration of 6.7 μM. The sample's extinction spectrum was measured following each immersion after it was rinsed in PBS and deionized water, and dried under nitrogen flow.

To ensure that the binding between rIgG and 11-AUT is stable, a second functionalized sample was immersed in 1 mM PBS solution for 1 hour, and an extinction spectrum was measured after the sample was rinsed and dried. This same sample was then immersed in 1.06 μM polyclonal (rabbit) anti-goat immunoglobulin G (anti-gIgG) for 1 hour to investigate the selectivity of the sensor. An extinction spectrum was measured after the sample was rinsed and dried. Finally, the sample was placed in a 1.06 μM solution of anti-rIgG for 1 hour to ensure that the sample was still sensitive to anti-rIgG. The sample was rinsed and dried before an extinction measurement was taken.

All of the immunoglobulin solutions used in this study were obtained from MP Biomedicals, LLC. (Solon, Ohio). The biosensor extinction measurements were taken with the sample in air.

3 DISCUSSION

The films consisted of a dense collection of silver nanoparticles, as shown in the top-view scanning electron microscopy (SEM) image in Fig. 1a. The majority of the particles are spherical and have diameters ranging from approximately 20 to 300 nm. Figure 1b shows an SEM image of the film cross-section, from which the nominal thickness of the film is determined to be approximately 150 nm. This is in contrast to previous LSPR studies using ultrathin silver and gold island films evaporated or sputtered at normal incidence [2, 3, 6, 8, 19, 20], where the film thickness

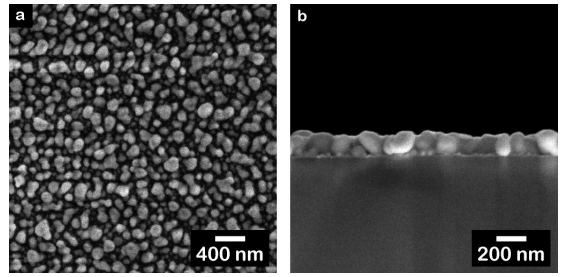

Figure 1: Scanning electron microscopy images of (a) the top surface, and (b) the cross-section of the Ag nanoparticle film.

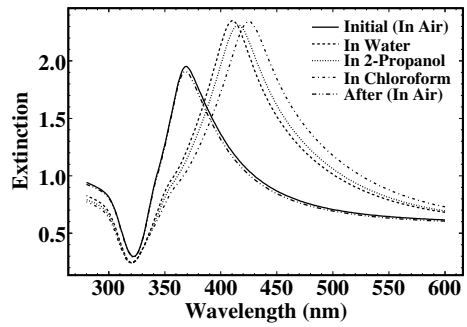

Figure 2: Extinction spectra in air before solvent measurements, in solvents of varying index of refraction, and in air again after the solvent measurements.

is limited to only a few nanometers. Here, the maximum film thickness is not limited by island aggregation and coalescence due to the self shadowing effect during GLAD film growth. The GLAD technique also allows for the density of the film to be easily controlled by adjusting the deposition angle, α. Finally, the shape of Ag nanoparticles produced by GLAD is not limited to spheres. Other groups using the GLAD technique or oblique angle deposition have demonstrated the growth of prolate silver nanoparticles and tilted silver nanorod arrays with polarized optical absorbance and surface enhanced Raman spectra [7, 14, 15, 21–23]. For this initial study on LSPR biosensors using GLAD, a simple vertical column structure was used. More complex structures that may provide enhanced biosensor performance are currently under investigation.

Prior to sensitivity measurements or sample functionalization, the samples were allowed to soak in deionized water for 24 hours. This treatment was found to stabilize the extinction spectra of the films upon subsequent immersion in solvents. The UV-visible extinction spectrum of the silver films in air exhibits a strong peak around a wavelength of 368 nm due to the LSPR.

To investigate the dependence of the LSPR peak extinction wavelength on the refractive index of the surrounding medium, the extinction spectra were measured

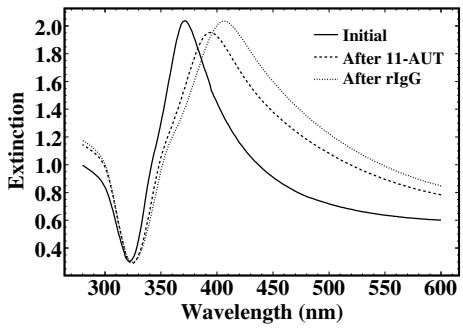

Figure 3: Extinction spectra before sample functionalization, and after the 11-AUT and rIgG functionalization steps.

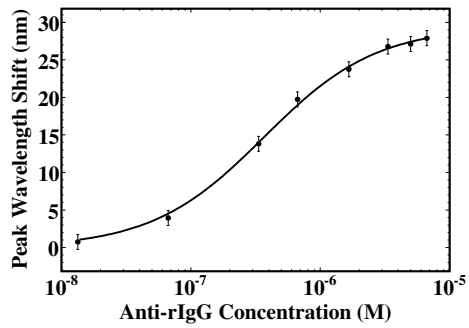

Figure 4: Peak LSPR extinction wavelength shift as a function of anti-rIgG concentration. The curve is a fit to the Langmuir isotherm given in Eq. 1. The error bars are estimates of the uncertainty in the wavelength shifts.

while a sample was immersed in liquids with varying refractive indices. The liquids used were deionized water, 2-propanol, and chloroform, with refractive indices of 1.33, 1.38, and 1.45, respectively. The wavelength shift of the extinction peak was found to be linearly dependent on the refractive index, with a wavelength shift per refractive index unit (RIU), or sensitivity factor, of 123 $\pm$ 3 nm/RIU and an R^2 value of 0.9998. This linear dependence has been reported by many groups and the sensitivity factor is comparable to reported values [11–13, 24]. After each measurement in solution, the sample was dried and a measurement was made with the sample in air to ensure the peak position returned to its initial value. The peak position consistently returned to within 2 nm of the initial spectrum peak, while the peak intensity decreased only slightly after all the measurements in solution were complete. The initial spectrum in air, the extinction spectra in the different solutions, and the spectrum in air after the solution measurements are shown in Fig. 2.

In this study, the binding event between rIgG and anti-rIgG is detected. The increase in the local refractive index near the silver surface upon biomolecule adsorption causes shifts in the extinction peak position due to the refractive index dependence of the LSPR. To prepare the biosensors, the films were first functionalized with a self assembled monolayer of 11-AUT. This was followed by exposure to a solution rIgG, which was immobilized to the sensor surface by non-specific adsorption to the amino group of the 11-AUT. The extinction spectra of a sample before modification and after each functionalization step is shown in Fig. 3. The peak extinction before modification occurred at a wavelength of 371 nm. After modification with 11-AUT and rIgG, the peak red-shited by 22 nm and a further 13 nm, respectively.

The functionalized films were able to detect the binding of anti-rIgG. An antibody capture binding curve was measured to test the sensors' functionality, as shown in Fig. 4. The sensor was exposed to different concentrations of anti-rIgG, [anti-rIgG], and the resulting peak wavelength shift, $\Delta\lambda$, was measured. The data in Fig. 4 was fit with the Langmuir isotherm:

$$\Delta\lambda = \Delta\lambda_{max} \frac{K_a\,[\text{anti-rIgG}]}{1 + K_a\,[\text{anti-rIgG}]} \tag{1}$$

where $\Delta\lambda_{max}$ is the saturation value of the extinction peak wavelength shift, and K_a is the surface-confined thermodynamic affinity constant. The wavelength shift was calculated in reference to the peak wavelength after the sample was functionalized with 11-AUT and rIgG. The saturation value, $\Delta\lambda_{max}$, and the affinity constant, K_a, were used as fit parameters, and were determined to be $\Delta\lambda_{max} = 29.4 \pm 0.7$ nm and $K_a = (2.7 \pm 0.3) \times 10^6$ M^{-1} by the minimization by a gradient (MIGRAD) method provided by the ROOT data analysis package [25]. The peak wavelength shift at a concentration of 6.7 μM was 28 $\pm$ 1 nm, which is close to the calculated saturation value. The K_a value determined here is comparable to that determined for similar IgGs with SPR imaging [26]. With respect to detection limit, we estimate that the minimum wavelength shift observable is approximately 2 nm. From the data collected in Fig. 4, this corresponds to 27 nM of the antibody. We expect improved detection limits with optimized film structures.

To ensure the binding of rIgG to 11-AUT is stable, a sample that was functionalized with 11-AUT and rIgG was soaked in 1 mM PBS for 1 hour, and a spectrum was measured after rinsing and drying the sample. The peak position was quite stable and blue-shifted by less than 1 nm. To test the response of the films to non-specific binding, the same sample was exposed to a 1.06 μM solution of anti-goat IgG for 1 hour. This resulted in a peak wavelength shift of about +1 nm. Finally, the sample was soaked in 1.06 μM of anti-rIgG for 1 hour to verify that the biosensor surface remained active after anti-gIgG exposure. This resulted in a peak shift of +17 nm. Thus, the sensor is responding to the specific binding between anti-rIgG and rIgG with a limited

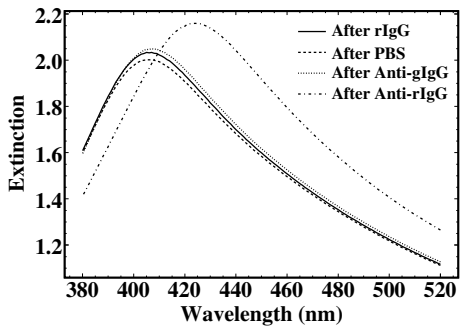

Figure 5: Extinction spectrum of rIgG functionalized sample, and spectra after incubation in 1 mM PBS, 1.06 μM anti-gIgG, and 1.06 μM anti-rIgG.

response to non-specific binding. The response of the sample to anti-rIgG was slightly less than the expected value of 22 nm from the fit to the data in Fig. 4b, which indicates a slight loss in sensitivity after exposure to the PBS and anti-gIgG solutions. Figure 5 shows the extinction spectra of the functionalized sample before and after exposures to the 1 mM PBS, 1.06 μM anti-gIgG and 1.06 μM anti-rIgG.

4 CONCLUSION

Localized surface plasmon resonance based biosensors were prepared using silver nanostructured films fabricated by glancing angle deposition. These films exhibited an extinction peak due to the LSPR, the position of which was linearly dependent on the refractive index of the surrounding medium. Functionalization of the films with 11-AUT and rIgG enabled the detection of specific anti-rIgG binding. The response to non-specific binding was investigated by exposing a functionalized film to anti-gIgG. This study has demonstrated the feasibility of using silver nanoparticle films fabricated by GLAD for LSPR based biosensing. The advantages of GLAD include the ability to produce large area silver nanoparticle films in a one-step deposition process at low cost, without the film thickness being limited by island aggregation and coalescence. However, improvements to the sensor properties are needed. The ability to control the film density and nanoparticle shape by the GLAD process may allow for the optimization of these properties.

Acknowledgments

The authors are grateful for support from the Natural Sciences and Engineering Research Council of Canada (NSERC), the Informatics Circle of Research Excellence (iCORE), Micralyne Inc., Alberta Ingenuity, the National Research Council–Genomics and Health Initiative (NRC-GHI), and the NRC National Institute for Nanotechnology (NINT). The authors would like to thank George Braybrook for taking the SEM images.

REFERENCES

[1] U. Kreibig, M. Vollmer, "Optical Properties of Metal Clusters," Springer-Verlag, 1995.
[2] G. Kalyuzhny *et al.*, J. Phys. Chem. B 104, 8238-8244, 2000.
[3] G. Kalyuzhny *et al.*, J. Am. Chem. Soc. 123, 3177-3178, 2001.
[4] M.D. Malinsky, K.L. Kelly, G.C. Schatz, R.P. Van Duyne, J. Am. Chem. Soc. 123, 1471-1482, 2001.
[5] A. Haes, R. Van Duyne, J. Am. Chem. Soc. 124, 10596-10604, 2002.
[6] M. Lahav, A. Vaskevich, I. Rubinstein, Langmuir 20, 7365-7367, 2004.
[7] S.B. Chaney, S. Shanmukh, R.A. Dluhy, Y.P. Zhao, Appl. Phys. Lett. 87, 031908, 2005.
[8] I. Doron-Mor *et al.*, Chem. Eur. J. 11, 5555-5562, 2005.
[9] H.K. Park, J.K. Yoon, K. Kim, Langmuir 22, 1626-1629, 2006.
[10] Y. Yang, L.M. Xiong, J.L. Shi, M. Nogami, Nanotechnology 17, 2670-2674, 2006.
[11] T. Arai, P.K.R. Kumar, K. Awazu, J. Tominaga, Mater. Res. Soc. Symp. Proc. 915, 0915-R02-08, 2006.
[12] I. Tanahashi, F. Yamazaki, K. Hamada, Chem. Lett. 35, 454-455, 2006.
[13] S. Malynych, G. Chumanov, J. Opt. A: Pure Appl. Opt. 8, S144-S147, 2006.
[14] Y.P. Zhao, S.B. Chaney, S. Shanmukh, R.A. Dluhy, J. Phys. Chem. B 110, 3153-3157, 2006.
[15] M. Suzuki *et al.*, Appl. Phys. Lett. 88, 203121, 2006.
[16] K. Robbie, M.J. Brett, A. Lakhtakia, Nature 384, 616, 1996.
[17] K. Robbie, M.J. Brett, J. Vac. Sci. Technol. A 15, 1460-1465, 1997.
[18] K. Robbie, M.J. Brett, United States Patent 5,866,204, 1999.
[19] R.P. Vanduyne, J.C. Hulteen, D.A. Treichel, J. Chem. Phys. 99, 2101-2115, 1993.
[20] G. Xu, M. Tazawa, P. Jin, S. Nakao, Appl, Phys. A 80, 1535-1540 2005.
[21] J.L. Martínez, Y. Gao, T. Lópezríos, Phys. Rev. B: Condens. Matter 33, 5917-5919, 1986.
[22] J.L. Martínez, Y. Gao, T. Lópezríos, A. Wirgin, Phys. Rev. B: Condens. Matter 35, 9481-9488, 1987.
[23] M. Suzuki *et al.*, Jpn. J. Appl. Phys. Part 2 44, L193-L195, 2005.
[24] T.R. Jensen *et al.*, J. Phys. Chem. B 103, 9846-9853, 1999.
[25] R. Brun, F. Rademakers, Nucl. Instrum. Methods Phys. Res. A 389, 81-86, 1997.
[26] V. Kanda, J. Kariuki, D. Harrison, M. McDermott, Anal. Chem. 76, 7257-7262, 2004.